

1 **Developments of Theories of Avian Movement Strategies in Wind and Their**
2 **Validation with Bio-logging Data**

3
4
5 Yusuke Goto^{1*}, and Ken Yoda¹
6

7 ¹*Graduate School of Environmental Studies, Nagoya University, Furo, Chikusa, Nagoya,*
8 *Japan.*
9

10
11 Animal movement represents an interdisciplinary research field
12 involving ecology and physics. Animal locomotion is composed of
13 three interrelated hierarchies: micro-scale mechanisms of
14 locomotion, often in the realm of physics; intermediate-scale
15 regulation of speed and direction and macro-scale movement of
16 route selection, those can significantly affect the fitness of the
17 animal. Based on these hierarchies, animal movement strategies
18 can be formulated as optimisation problems, yielding some
19 theoretical predictions that can now be tested using bio-logging
20 techniques to record animal movements. This review focuses on
21 bird movement strategies in response to wind and aims to provide
22 a practical overview of how theory and empirical testing with bio-
23 logging data are carried out in the field of movement ecology.
24

25 **1. Introduction**

26 Animal movement is an area of research that spans two different fields: ecology and
27 physics. The elucidation of the wide variety of movement mechanisms exhibited by
28 animals on land, in water, and in the air is the realm of physics [1–6]. In particular, the
29 study focusing on detailed spatio-temporal scale animal movements and the mechanical
30 mechanisms that produce them is often referred to as biomechanics. On the other hand,
31 real animals in the wild move over much broader scales than those studied in indoor
32 experiments. How such movements affect the ecology and evolution of wild animals (e.g.,
33 food acquisition, survival, reproductive success, population dynamics, species
34 distribution, etc.) is one of the central issues in ecology, and in recent years the research
35 field dealing with this topic has been called movement ecology [7].

36 Biomechanics is often interested in the micro-scale mechanisms of animal
37 movement, while movement ecology is interested in the intermediate-scale regulation of
38 speed and direction of movement and the larger-scale movement of route selection, yet
39 animal movement is composed of these three interrelated hierarchies (Fig. 1). First, if we
40 focus on macro-scale movement, the route from an animal's starting point to its goal,
41 costs such as time, energy, and risk of mortality to reach the destination will affect the
42 fitness of the animal through its survival and reproductive success. Since the costs

43 associated with movement are influenced by internal factors such as morphology,
44 cognitive ability, and experience, as well as external factors such as food distribution
45 along the route and wind, animals are expected to select the route that lowers costs
46 according to these factors. The travel route is the result of the integration of the travel
47 direction and speed of the intermediate-scale animal at each time, and the energy
48 consumption rate at each time can be formulated as a function with travel speed and
49 direction as variables, due to the physical mechanism of movement at the micro-scale.
50 Thus, animal route selection can be attributed to the optimization problem of finding a
51 route that minimizes the objective function (energy consumption), and the optimal
52 solution can be employed as testing hypotheses [8]. The approach of formulating animal
53 behavior into optimization problems, deriving testing hypotheses, and examining them
54 using real data has been standard in behavioral ecology [9–12], and pioneering
55 theoretical studies on wind-dependent migration strategies of flying animals, the focus of
56 this review, were already conducted in the late 1970s [13,14].

57 Until the 1970s and 1980s, the available wildlife movement data for testing
58 these theories was mainly based on rough spatiotemporal resolution, such as visual
59 and/or radar-based fixed-point observations and marked recapture information [15,16].
60 Subsequently, however, the development of behavior recorders that can be attached to
61 birds has made it possible to record routes of wild animals over long periods starting with
62 studies on large birds [17,18] followed by a variety of species of different sizes. Various
63 parameters can also be measured, including acceleration [19,20], video [21–23], attitude
64 angle [24–27], heart rate [28,29], and neural activity [30,31]. This method of acquiring
65 behavioral data by attaching behavior loggers to wild animals is called bio-logging.

66 This review is targeted at physicists interested in animal movement and bio-
67 logging data and will review the classical theories of animal movement and their
68 validation with real data, focusing on the bird's movement strategy in response to wind.
69 Among animal movements, there are three reasons for limiting the topic to the movement
70 of birds in response to wind. First, bird flight is governed by physical laws that allow us
71 to construct a model linking travel speed and energy consumption. Second, among the
72 animal kingdom, birds are one of the most widely studied groups for bio-logging studies.
73 Finally, wild animals encounter a variety of wind environments due to habitat differences
74 among species and environmental changes during their travel, and thus the manipulation
75 experiments that alter wind environments are conducted in nature, and birds' responses
76 to wind in these different situations can be useful for inferring their migratory abilities,
77 cognitive abilities, and movement strategies.

78

79 **2. Optimization Problem Formulation of Bird Navigation Strategies in Response**
80 **to Wind**

81 This section outlines the interrelation among the three hierarchies that constitute animal
82 navigation, as depicted in Figure 1. Prior to delving into the main theme, we bring forth
83 two noteworthy aspects, namely the explication of terminologies and the flight styles of
84 avian species.

85

86 **2.1 Air Velocity and Ground Velocity**

87 Here, we explicate the air and ground velocity (Figure 2). The velocity, which is defined
88 as a vector that incorporates both speed and direction, of a bird with respect to the
89 ground is referred to as the ground velocity. Its magnitude is termed as the ground speed,
90 and its direction is referred to the direction of motion in this review. The velocity of the
91 bird with respect to the air is called as the air velocity. The air velocity is the resultant
92 vector obtained by subtracting the wind velocity from the ground velocity. The magnitude
93 of air velocity is defined as airspeed. In the field of animal behavior, the direction of the
94 air velocity is frequently called as the "heading direction" [32], a convention upheld in this
95 paper. It should be noted that the heading direction may not necessarily coincide with
96 the direction of the bird's body axis. However, the difference between the two is often
97 assumed to be small enough to be identical [33], and thus this review will not distinguish
98 between them in the following. A notation of the symbols in this review is listed in Table
99 1.

100

101 **2.2 Flapping Flight and Soaring Flight**

102 Avian flight can be divided into two main categories: flapping flight, in which birds move
103 their wings to stay aloft, and gliding flight, in which they remain airborne without wing
104 movement. Among gliding flights, soaring is a flight style that utilizes wind energy and is
105 primarily observed in larger birds. The two major types of soaring flight are thermal
106 soaring, which exploits updrafts [25,34–36], and dynamic soaring, which utilizes wind
107 speed difference with altitude [33,37–42]. Although the focus of our review is on flapping
108 flight, the theoretical framework presented here is also applicable to understanding
109 movement strategies in soaring flight. For readers interested in learning more about
110 movement strategies in soaring flight, we suggest consulting the references cited above
111 as well as references [43–45].

112

113 **2.3 Bird Movement Strategies in Response to Wind and Three Levels of Layers**

114 The movement mechanism constitutes the first layer in the avian navigation hierarchy.

115 During sustained wing-flapping flight at a constant altitude, a bird's energy consumption
 116 rate (P) is inherently associated with its airspeed (V), due to the fundamental physical
 117 principles that govern avian flight.

118

$$119 \quad P(V(t)) \quad (1)$$

120

121 $V(t)$ is the airspeed at time t . The graph of P with V as a variable shows a U-shape (see
 122 next section).

123 Next, to consider the second and third layers of bird navigation hierarchy, we
 124 consider the cost of travel. The animal's position at time t , $\vec{X}(t)$, is given by

125

$$126 \quad \vec{X}(t) = \int_{t_0}^t (\vec{V}(\tau) + \vec{W}(\vec{X}(\tau), \tau)) d\tau + \vec{X}(t_0) \quad (2)$$

127

128 where $\vec{W}(\vec{X}(t), t)$ is the wind velocity at time t at the bird's position $\vec{X}(t)$. The energy
 129 consumed by the animal as it moves from time t_0 to t is given by

130

$$131 \quad E(t, t_0) = \int_{t_0}^t P(V(\tau)) d\tau \quad (3)$$

132

133 The energy expended by an animal per unit distance traversed" is denoted as the cost
 134 of transport (COT). This quantity is frequently employed in movement ecology to develop
 135 theoretical frameworks for animal locomotion, with COT serving as the objective function
 136 that animals are hypothesized to minimize during their travel. The COT between time t_0
 137 and t is formulated as follows.

138

$$139 \quad c(t, t_0) \equiv \frac{E(t, t_0)}{|\vec{X}(t) - \vec{X}(t_0)|} \quad (4)$$

140

141 By employing the COT as the currency of locomotion, predictions on animal movement
 142 can be made. It should be noted that in this review, COT is adopted as the currency of
 143 movement. Depending on the circumstances of the animals in question, alternative
 144 quantities may be more suitable as the currency. Nevertheless, even in such cases, the
 145 framework outlined in this review can be applied by replacing the objective variable.

146 Next, we move on to the second layer of the animal navigation hierarchy, which concerns
 147 the adjustment of airspeed and heading. Firstly, we demonstrate that the airspeed that

148 minimizes the COT can be deduced from the constraint $P(V(t))$ provided in the first layer.
 149 Let us suppose that an animal moves with a heading angle of θ during a short time
 150 interval of Δt . Under such circumstances, the COT from time t to $t+\Delta t$ can be defined as
 151 follows.

$$152 \quad \mathcal{C}(t) \equiv \lim_{\Delta t \rightarrow 0} \overline{c(t + \Delta t, t)} \quad (5)$$

154
 155 The following equation is obtained from the definition and eq (3) and (4).

$$156 \quad \mathcal{C}(t) = \lim_{\Delta t \rightarrow 0} \frac{E(t + \Delta t, t)}{|\overline{\mathbf{X}}(t + \Delta t) - \overline{\mathbf{X}}(t)|}$$

$$157 \quad \cong \lim_{\Delta t \rightarrow 0} \frac{P(V(t))\Delta t}{|\overline{\mathbf{X}}(t + \Delta t)/\Delta t - \overline{\mathbf{X}}(t)/\Delta t|\Delta t}$$

$$158 \quad = \frac{P(V(t))}{|\overline{\mathbf{V}}(t) + \overline{\mathbf{W}}(\overline{\mathbf{X}}(t), t)|}$$

$$159 \quad = \frac{P(V(t))}{V_g(t)} \quad (6)$$

160
 161 Here $V_g(t)$ represents the ground speed at time t . Hence, the airspeed that minimizes
 162 $\mathcal{C}(t)$ is deduced from

$$163 \quad \frac{\partial \mathcal{C}(t)}{\partial V} = \frac{\partial}{\partial V} \left(\frac{P(V(t))}{|\overline{\mathbf{V}}(t) + \overline{\mathbf{W}}(\overline{\mathbf{X}}(t), t)|} \right) = 0. \quad (7)$$

164
 165 The airspeed that minimize the COT is called as maximum range speed (V_{mr}). The V_{mr}
 166 is dependent on both the heading angle and wind velocity. While we have provided the
 167 values of θ a priori, the question remains: in what direction should the bird orient its
 168 heading direction to minimize COT? In the absence of a specific goal location, as occurs
 169 when birds search for unpredictable food sources, it is advantageous to move in a
 170 direction that maximizes the distance traveled per unit of energy expended. Such a
 171 direction of movement can be derived from $\frac{\partial \mathcal{C}(t)}{\partial \theta} = 0$ and $\frac{\partial \mathcal{C}(t)}{\partial V} = 0$.

172 In the presence of a target location, the orientation strategy of birds is commonly
 173 classified based on three directions: the direction of travel, the direction of the wind, and
 174 the preferred direction in which the bird intends to progress. If the speed and direction of
 175 the wind remain constant, birds can minimize their energy expenditure by taking a

179 straight path towards the goal by offsetting the crosswind, a strategy known as complete
 180 compensation. However, if the bird's airspeed is slower than the crosswind, or if it is
 181 unable to accurately determine the direction of the distant goal, the direction of
 182 movement will deviate from the goal direction due to the crosswind, which is referred to
 183 as drift.

184 Some avian species exhibit migratory behavior, moving between breeding and
 185 wintering grounds during the spring and fall seasons, with some covering thousands of
 186 kilometers. On such extended spatial scales, wind patterns frequently exhibit spatial
 187 variability. In such a situation, selecting a detour route that leverages favorable tailwind
 188 assistance can result in a lower energy expenditure compared to a straight route to the
 189 destination. Suppose the bird leaves \vec{X}_{start} at time $t = 0$, travels along path l , and arrives
 190 at its goal position \vec{X}_{goal} at time $t = T$.

191

$$192 \quad \vec{X}_{goal} = \int_0^T (\vec{V}(\tau) + \vec{W}(\vec{X}(\tau), \tau)) d\tau + \vec{X}(0) \quad (8)$$

193

194 The energy expended, denoted by E_l , during this travel can be obtained by integrating
 195 COT along the path l . By converting the integrating variable to time, E_l can also be
 196 expressed as the time integral of power.

197

$$198 \quad E_l = \int_l C(t) ds$$

$$199 \quad = \int_0^T P(V(\tau)) d\tau \quad (9)$$

200

201 $\int_l * ds$ denotes the integration of a variable $*$ along the curve l . Therefore, the optimal
 202 path selection problem can be reduced to a functional minimization problem, where we
 203 seek to find a function $\vec{V}(t) (0 \leq t \leq T)$ and the travel time T that minimize the energy
 204 functional E_l subject to the constraint eq (1). The optimal path can be obtained by
 205 integrating $\vec{V}(t)$.

206

207 In this section, we have presented the relationship between the three
 208 hierarchies without delving into the specific functional forms of power and COT. Now,
 209 then, what specific predictions can be derived from the formulations and assumptions
 210 described here? In the following sections, we will give concrete form to these functions
 and review the movement strategies predicted from this framework and their examination

211 with real data.

212

213 **3. Relationship Between Flight Speed and Power**

214 In this section, we examine the relationship between avian flight speed and energy
215 consumption, as well as the underlying physical mechanisms. The key takeaway is that
216 the energy consumption rate (P) for birds flying at a constant altitude and airspeed (V)
217 follows a U-shaped function, with V as the independent variable. This function is called
218 the power curve.

219

220

$$221 \quad P(V) = a_1 + \frac{a_2}{V} + a_3V^3 \quad (10)$$

222

223 **3.1 Power Curve**

224 Here, we examine a scenario in which a bird is consistently flying at a constant airspeed
225 V and fixed altitude by flapping its wings. It is important to note that the airflow around a
226 bird in flight through wing flapping is highly complex and challenging to fully comprehend.
227 Therefore, we employ a rough approximation and consider the averaged vertical and
228 forward forces generated by the bird over a duration that is sufficiently longer than a
229 single flap. To remain airborne, birds must maintain equilibrium between the upward force
230 produced by wings and the gravitational force acting upon them. Furthermore, they must
231 also balance the forward force with the drag force that acts in the direction opposite to
232 the air velocity. Hence, the powers required for flight can be expressed as a function of
233 airspeed (see [46] for detailed derivation). These powers are categorized as induced
234 power, P_{ind} , parasite power, P_{par} , and profile power, P_{pro} .

235 The induced power is the power needed to generate lift that counters the
236 gravitational force. In the case of a bird with a wingspan of b in flight, the required power
237 P_{ind} , to maintain a constant airspeed of V while interacting with the air passing through
238 a circular area with a diameter of b , and to transfer momentum to the air to offset the
239 force of gravity, can be given by [46],

240

$$241 \quad P_{ind} = \frac{2k(mg)^2}{\pi b^2 \rho V}. \quad (11)$$

242

243 The bird's mass is denoted by m , while b represents the wingspan, and ρ represents the
244 density of the atmosphere. The induced power factor, k , is a constant that accounts for
245 the deviation from a perfect circle in the region where the bird interacts with the air, and

246 is often taken to be 1.2 [44]. The drag force on the body is called parasite drag and is
247 given by

248

$$249 \quad D_{par} = \frac{1}{2} \rho S_b C_{D,par} V^2 \quad (12)$$

250

251 where $C_{D,par}$ is called parasite drag coefficient. The S_b is the cross-sectional area of
252 the body of an animal when viewed from the front called frontal body area. P_{par} is
253 product of the parasite drag and the airspeed.

254

$$255 \quad P_{par} = \frac{1}{2} \rho S_b C_{D,par} V^3 \quad (13)$$

256

257 In addition to the induced drag that creates lift, the wing also experiences drag due to
258 pressure and friction, which is known as profile drag. The power required to counteract
259 this type of drag is denoted as P_{pro} . P_{pro} has more uncertainties than P_{ind} and P_{par} ,
260 and several different models have been proposed. The P_{pro} depends on the airflow
261 passing over the bird's wing which can be separated into two components: one due to
262 the bird's forward motion and the other due to the flapping motion. As the former
263 component increases in proportion to the airspeed, while the latter component decreases
264 in proportion to airspeed as a result of decreasing flapping frequency and amplitude, [44]
265 assumed that the profile power is constant at the typical airspeed at which birds fly.
266 Specifically, the minimum power required for an "ideal bird" without profile power,
267 denoted as $\min_V(P_{ind} + P_{par})$, is determined, and the profile power is then assumed to be
268 a constant multiple of this power.

269

$$270 \quad P_{pro} = \frac{C_{pro}}{AR} \min_V(P_{ind} + P_{par}) \quad (14)$$

271

272 AR is the aspect ratio (wingspan squared divide by wing area), and C_{pro} is called the
273 "profile power constant" and a value of 8.4 has been adopted [44]. On the other hand,
274 [41] assumed that P_{pro} depends on V [47].

275

$$276 \quad P_{pro} = \frac{1}{2} \rho S_w C'_{D,pro} V^3 \quad (15)$$

277

278 These studies have simplified the effect of wing reciprocation on profile drag. However,

279 a recent study [48] has quantified the impact of wing kinematics on profile drag and
280 developed an R package called `afpt` that is able to calculate a power curve based on this.
281 The sum of the three powers, namely P_{ind} , P_{par} , and P_{pro} , yields the mechanical power,
282 P_{mec} , required for flapping flight.

283

$$284 \quad P_{mec} = P_{ind} + P_{par} + P_{pro} \quad (16)$$

285

286 To produce this mechanical power, the bird must activate its muscles, lungs, and
287 circulatory system. Moreover, energy expenditure by basal metabolism also occurs.
288 Hence, in order to determine the chemical power (P) required by the bird to generate
289 P_{mec} , it is necessary to take into account the energy conversion efficiency of the muscles,
290 the energy consumption of the lungs and circulatory system, as well as basal metabolism
291 [44].

292

$$293 \quad P = R \left(\frac{P_{mec}}{\epsilon} + M_B \right) \quad (17)$$

294

295 M_B represents the organism's basal metabolic rate. The dimensionless parameter ϵ ,
296 which is commonly assigned a value of 0.23 [44], denotes the efficiency of converting
297 mechanical power into the power generated by the flight muscles. The dimensionless
298 parameter R , which is often assigned a value of 1.1 [44], accounts for the additional
299 power required to operate the respiratory and circulatory systems. Both P_{mec} and P are
300 dependent on the airspeed, and their respective curves are referred to as power curves
301 (to differentiate between the two, the former is sometimes called the mechanical power
302 curve). Although the values of parameters used in the assumed power curve and the
303 functional form of the profile power may differ across studies, based on the previous
304 discussion, it is expected that the power curve can be approximated using Equation
305 (10) and has the qualitative characteristic of being U-shaped with respect to the
306 airspeed V .

307 To what extent does this theoretical power curve accurately depict the actual
308 one? Although measuring power curves poses technical challenges, [49] demonstrated
309 that the mechanical power curves of cockatiels and ringed turtle-doves are U-shaped
310 by quantifying the momentum these species impart on the surrounding air while flying
311 within a wind tunnel. This was achieved by simultaneously measuring the length and
312 force of their pectoralis muscles, in addition to the three-dimensional motion of their
313 wings and bodies. In 2003, Particle Image Velocimetry (PIV) technology, a laser beam-

314 based method for quantifying airflow around a wing by tracking the motion of particles,
315 was incorporated into animal flight research [50,51]. Subsequent studies have
316 documented U-shaped power curves in birds, bats, and moths [52–54]. However, it is
317 noteworthy that, although pied flycatchers exhibit a U-shaped power curve, that is
318 flatter than the theoretical prediction as demonstrated by [53]. This is due to the
319 parasite power changing as the bird's body pitch direction changes with airspeed.
320 Overall, the qualitative features of the U-shaped power curve are supported by many
321 studies, but the quantitative value may not agree with the predictions of classical
322 theory. In subsequent sections, we will show that predictions of bird movement
323 strategies can be classified into two types: quantitative predictions using the values of
324 the power curve itself and qualitative predictions using the U-shaped nature of the
325 power curve, but we note here that qualitative predictions are more robust against
326 power curve uncertainty.

327

328 **4. Speed Adjustment and Orientation**

329 In this section, we investigate how avian species adjust their airspeed and heading in
330 response to wind conditions, operating under the assumption that the cost of transport
331 (COT) is minimized at the given moment. We commence by discussing the concept of
332 minimum power speed and maximum range speed, employing power curves as the
333 foundation of our analysis. Subsequently, we propose a theoretical prediction on how the
334 maximum range speed is influenced by the wind direction in relation to the bird's travel
335 direction, and present research studies that have empirically tested this prediction using
336 bio-logging data. The derivation of the maximum range speed assumes that the bird is
337 perfectly oriented in its intended travel direction. However, in reality, crosswinds can
338 induce drift, causing the animal's trajectory to deviate from its intended path. In the latter
339 part of this section, we will delve into the categorization of bird orientation and the
340 underlying factors that contribute to the orientation strategy birds employ, and review
341 empirical studies.

342

343 **4.1 Minimum Power Speed and Maximum Range Speed**

344 The airspeed that minimizes power during flight is referred to as the minimum power
345 speed, whereas the airspeed that minimizes the cost of transport (COT) is known as the
346 maximum range speed. Initially, we will explore these speeds under windless ($V = V_g$)
347 conditions. For the sake of simplicity, we shall omit the notation of time of each variable.
348 The minimum power speed is the velocity that minimizes $P(V)$, and the maximum range
349 speed is the speed (V) that minimizes

350

351

$$c = \frac{P(V)}{V}. \quad (18)$$

352

353 As c is the slope of the power curve, it can be visually inferred that the point of tangency
354 between the power curve and the origin corresponds to the maximum range speed (Fig.
355 3). Since the maximum range speed demands lower energy expenditure for covering the
356 same distance compared to the minimum power speed, it is generally expected for
357 animals to adopt the former. However, species with limited power production capabilities
358 may opt for an airspeed closer to the minimum power speed due to the higher energy
359 requirement per unit of time associated with maximum range speed. Shags exhibit dual
360 locomotion capabilities, encompassing both diving and flying. However, the distinct
361 morphological adaptations required for these two forms of locomotion give rise to trade-
362 offs in their overall morphology. Kerguelen shags possess a specialized morphology for
363 diving, characterized by a higher body mass, shorter wings, and smaller flight muscles.
364 These adaptations may limit their flight performance as a consequence of such trade-
365 offs. A study [55] revealed that the average flight time of this species is only 24 minutes
366 per day. Furthermore, the study measured the airspeed of Kerguelen shags and
367 compared it with the theoretical estimates of minimum power speed and maximum range
368 speed. The findings indicated that the airspeed of this species is closer to the minimum
369 power speed rather than the maximum range speed. Hence, it can be inferred that the
370 morphological characteristics of this species are not conducive to generating the
371 necessary power for achieving the maximum range speed, which enables greater
372 distance to be covered per unit of energy consumed but requires higher energy
373 expenditure per time as compared to the minimum power speed.

374

375 **4.2 Maximum Range Speed in the Presence of Wind**

376 Next, consider the maximum range speed in the presence of wind [56]. The COT is given
377 as

378

379

$$c = \frac{P(V)}{V_g} = \frac{P(V)}{|\vec{V} + \vec{W}|} \quad (19)$$

380

381 Let α be the angle that the air velocity makes with the ground velocity and let β be the
382 angle that the wind velocity makes with the ground velocity (Fig. 2). Then ground speed
383 is represented as the following.

384

$$385 \quad V_g = W \cos \beta + \sqrt{V^2 - (W \sin \beta)^2} \quad (20)$$

386

387 V that minimizes \mathcal{C} satisfies the following.

388

$$389 \quad \frac{\partial \mathcal{C}}{\partial V} = \frac{\partial}{\partial V} \left[\frac{P(V)}{W \cos \beta + \sqrt{V^2 - (W \sin \beta)^2}} \right] = 0 \quad (21)$$

390

391 From the above equation, the following results are obtained.

392

$$393 \quad \frac{\partial P}{\partial V} = \frac{P}{V_g \cos \alpha} \quad (22)$$

394

395 For simplicity, let us consider the situation where there is no crosswind component ($\alpha =$
396 0). In this case, the above equation is

397

$$398 \quad \frac{\partial P}{\partial V} = \frac{P}{V_g}. \quad (23)$$

399

400 The airspeed that satisfies the given equation can be comprehended visually from the
401 power curve plots. In Fig. 3, the maximum range speed is depicted for both tailwind (the
402 orange line) and headwind conditions (the blue line). As observed from the diagram, the
403 maximum range speed is greater for headwind and lower for tailwind compared to the
404 no-wind condition. In the presence of a crosswind component, the airspeed is influenced
405 by two variables: wind speed and wind direction. By taking into consideration the
406 relationship between wind speed and maximum range speed, it can be noted that when
407 the wind is a tailwind ($\beta = 0^\circ$), the maximum range speed decreases proportionally with
408 the wind speed. On the other hand, when the wind becomes a headwind ($\beta = 180^\circ$), the
409 relationship between wind speed and maximum range speed reverses, with higher wind
410 speeds resulting in higher maximum range speeds, see [56] for detail.

411

412 The modulation of airspeed in response to the wind conditions by avian species
413 has been investigated utilizing radar and bio-logging data. For instance, radar
414 measurements of airspeed for migratory birds at 12 stations along the Northwest
415 Passage in the Arctic region of Canada have reported a reduction in airspeed in response
416 to the strength of the tailwind component [57]. The observation of the movement of
migrating Arctic terns, employing binoculars equipped with three integrated sensors

417 including a laser range finder, a magnetic compass, and an elevation angle sensor, has
418 revealed a decrease in airspeed for this species in correlation with an increase in the
419 tailwind component [58]. Furthermore, studies have indicated that the adjustment of
420 airspeed is also evident during foraging flights lasting several hours or minutes. Tracking
421 with GPS has demonstrated that species such as kittiwakes and shags modulate their
422 airspeed in accordance with the strength of the tailwind component [59,60].

423 It is noteworthy that we can investigate which airspeed, specifically the
424 minimum power speed or the maximum range speed, avian species adopt by examining
425 their adjustments in response to wind. The theoretical proposition posits that if birds
426 adopt the maximum range speed, they would modulate their airspeed based on wind
427 conditions. Conversely, if birds adopt the minimum power speed, their airspeed would
428 remain unchanged regardless of wind conditions, as the minimum power speed is
429 independent of wind. This qualitative prediction confers the advantage of being less
430 sensitive to uncertainties in parameters and profile power of the power curve, as
431 compared to quantitative predictions that calculate the values of the minimum power
432 speed and maximum range speeds from a power curve. [60] reported that European
433 shags breeding on the Isle of May in the U.K. adopt a maximum range speed, changing
434 their airspeed according to the strength of the tailwind component This is interesting
435 considering that Kerguelen shags, which dive and fly like European shags, adopt
436 maximum range speed [55]. This difference may suggest that the Kerguelen shag is
437 more focused on diving than flying. However, since [55] did not test for changes in
438 airspeed with tailwind strength, it may be an interesting issue to test whether airspeed
439 changes with wind for Kerguelen shags as well.

440 It has also been reported that animals modulate their airspeed not only in
441 response to the tailwind component, but also to the crosswind component during
442 migratory flights in common swifts [61] and foraging trips in bats [62]. [62] examined the
443 correlation between wind speed and airspeed, which exhibited variation with wind
444 direction (β) relative to the track direction, in a straw-colored fruit bat breeding in Ghana.
445 The GPS tracking data of this species was collected at 5-minute intervals, and combined
446 with a meteorological model that simulates local winds at a high spatio-temporal
447 resolution (1 km x 1 km mesh, 1 min). Air velocity was calculated from the GPS-recorded
448 ground velocity and the simulated winds to investigate how airspeed varies with wind
449 direction and speed. The results revealed that the relationship between airspeed and
450 wind speed changed with wind direction. In tailwind conditions ($\beta = 0$), airspeed
451 decreased with increasing wind speed, but as the wind direction shifted from oblique
452 back to headwind, airspeed increased with wind speed, and the rate of change of

453 airspeed with wind speed became more pronounced as the wind direction approached
454 headwind conditions ($\beta = \pi$). These results indicate that this species adjusts its airspeed
455 in response to both wind speed and wind direction, as predicted by theoretical
456 expectations.

457 The adjustment of airspeed may be constrained by environmental factors and
458 the cognitive ability of birds. [63] reported that during migration, common swifts do not
459 adjust their airspeed at high altitudes and during nighttime. This may be attributed to the
460 lack of visual cues available to the birds in these situations, making it difficult for them to
461 determine their airspeed relative to the cues, leading to unsuccessful regulation of
462 airspeed. Thus, theoretical predictions not only enable us to evaluate optimal animal
463 behavior, but also yield valuable insights into the cognitive acumen of avian species
464 through disparities between theoretical predictions and empirical observations.

465

466 **4.3 Adjustment of Heading Direction**

467 In the derivation of the maximum range speed, we have predetermined the heading angle
468 of an organism. However, which heading direction minimizes COT? If the wind remains
469 constant in space and time, extending from the starting point to the goal, the heading
470 angle that aligns the travel direction with the goal direction minimizes COT [14,64]. When
471 the travel direction aligns precisely with its intended destination to move, it is termed
472 'complete compensation' [32]. Nonetheless, actual avian navigation may not always
473 exhibit this orientation. Three potential factors could contribute to this deviation. Firstly,
474 limited airspeeds available to the bird may act as a constraint. Secondly, cognitive
475 limitations may impair the bird's ability to perceive its position and direction accurately
476 relative to the target. Thirdly, changes in wind patterns en route may hinder complete
477 compensation from minimizing the energy expended to reach the goal. Hence, it is crucial
478 to explore alternative modes of avian orientation beyond complete compensation.

479 When discussing the orientation of birds in response to wind, the focus often
480 centers on the interrelationships among four directions: bird heading direction, bird travel
481 direction, wind direction, and the Preferred Direction of Movement (PDM) [32,65,66].
482 PDM refers to the direction in which the bird intends to move at a specific location at time
483 point t ($\vec{X}(t)$). PDM is also commonly known as the "preferred goal direction", "preferred
484 track direction", or "intended direction of movement". It is important to note that the
485 definition of PDM can vary depending on the study. For example, in some instances,
486 PDM is defined as the direction of the bird's final goal point (\vec{X}_{goal}) as observed from
487 $\vec{X}(t)$ [32,67,68], whereas in other cases where there is a clearly identifiable migratory
488 stopover point, PDM is defined as the direction of that point as viewed from $\vec{X}(t)$ [69].

489 In these cases, researchers predefine the PDM. However, in other situations, PDM is
490 estimated from the data without making assumptions about the target point [65,70,71]. It
491 is therefore crucial to note how PDM is defined in each study.

492 [32] proposed that the relationship between heading direction, travel direction,
493 wind direction, and PDM can be classified into eight types (Fig. 4). Complete
494 compensation is one of these types, in which the travel direction coincides with the PDM.
495 In contrast, the state in which the heading direction coincides with the PDM, and travel
496 direction deviates from PDM due to crosswind, is called full drift. The state between
497 complete compensation and full drift is called partial compensation or partial drift. The
498 state where the travel direction is more upwind than the PDM is called overcompensation.
499 Compass downstream orientation is a compromise between speed and moving to the
500 PDM, where the animal slightly deviates the heading direction from the wind direction to
501 the PDM. Compass downstream orientation has the greatest deviation from the goal
502 compared to the four strategies listed earlier, but it can achieve the highest travel speed
503 if the airspeed is the same for all strategies. In these 5 orientation strategy has PDM,
504 while those without PDM include passive downstream transport, downstream orientation,
505 and upstream orientation. Passive downstream transport occurs when animals without
506 self-propulsion flight along with wind, like wind or water, and cannot control their speed
507 or direction. Active downstream orientation is when animals actively swim or fly in the
508 same direction as the flow to maximize their speed and travel distance. This strategy is
509 useful when speed and minimal energy consumption are more important than to reach a
510 specific goal point. It allows the animal to move faster, resulting in small COT, while still
511 moving in the preferred direction to some degree. Upstream Orientation is when animals
512 move directly against a flow, often seen in situations to find food and mates.

513

514 **4.4 Empirical Test of Orientation Strategies**

515 It may not always be obvious how to identify which orientation type a species falls under
516 from real bird movement data. This is because we do not always know the PDM of a bird.
517 For example, when birds return to their nests after foraging, their final destination is
518 definitely the nest, but they may take a detour to reach another stopover point along the
519 way before reaching the goal, and such a detour in homing has been reported in the
520 shearwaters [71,72] and Antarctic petrels [73]. [65] overcomes this difficulty and is often
521 used as a method to quantify the degree of wind compensation and PDM of a bird from
522 empirical data. This method allows for the estimation of bird compensation and PDM
523 from information on the ground velocity and wind velocity (and the air velocity obtained
524 from the difference between the two velocities) of multiple individual birds observed at a

525 given location. Specifically, the angle (α) between the air velocity vector and the ground
526 velocity vector is plotted on the x-axis, and the travel direction is plotted on the y-axis,
527 and a regression line is drawn. The slope of the regression line gives the orientation
528 information, and the intercept gives the PDM. The orientation of the species is classified
529 as complete compensation when (slope) = 0, full drift when (slope) = 1, partial
530 compensation when $0 < (\text{slope}) < 1$, over compensation when (slope) < 0, and compass
531 downstream orientation when (slope) > 1. Note that this analysis assumes that the
532 individuals used in the analysis have the same PDM. For details, please refer to the
533 original research [65].

534 In the following, we review some empirical investigations that explore the
535 influence of an animal's locomotive capabilities and cognitive faculties on its orientation
536 in responses to wind.

537 First, as a study showing that the airspeed that a species can achieve has a
538 strong influence on the orientation adopted by that species, there is an example of
539 comparing orientation among organisms with greatly different airspeeds they can
540 achieve [70]. This study analyzed thousands of radar tracking data from multiple spring
541 and fall migrations of songbirds flying over southern Sweden and *A. gamma* moths flying
542 over southern England in northwestern Europe and compared their orientation strategy.
543 Both studied moths and songbirds fly at night at high altitudes (200 to 800 m for moths
544 and 500 to 2,500 m for songbirds) and experience wind speeds of 6-22 m s⁻¹. Songbird
545 airspeed is 8-16 m s⁻¹ while moth airspeed is slower at 3-5 m s⁻¹, suggesting that moths
546 are expected to have less ability to compensate for crosswinds than birds. Indeed, moths
547 drifted more strongly than songbirds. However, interestingly, the mean ground speed of
548 moths was higher than that of songbirds. In other words, birds were able to reach the
549 goal position accurately, albeit at a slower ground speed than moths due to wind
550 compensation, whereas moths were able to reduce travel costs by actively using wind
551 assistance, albeit at the expense of reaching the target point accurately. Thus, the study
552 showed that each species employed an adaptive orientation strategy suited to its
553 locomotion capabilities.

554 Next, we review studies exploring the cognitive abilities of birds by examining
555 their orientation responses to wind. Discerning one's drift due to wind would conceivably
556 be more challenging for a species in environments lacking landmarks, such as oceanic
557 or desert regions, as opposed to terrestrial settings abundant in landmarks. Several
558 avian species predominantly traverse land and only undertake journeys across oceans
559 and deserts during migration. The capacity of these birds to compensate for crosswinds
560 while navigating over the sea was investigated through the employment of radar

561 technology. Some studies showed that the extent of compensation of terrestrial birds
562 decreases when navigating over the sea, in comparison to terrestrial environments. For
563 example cranes [16] and wood pigeons [74], show comprehensive compensation on land,
564 yet partial compensation during their flights across the sea. Compared to these species
565 that fly over the sea for short distances and time, the ability of wind compensation is
566 thought to have a greater impact on travel costs and mortality risk for land bird species
567 that migrate long distances at sea during migration. Recent bio-logging technology has
568 made it possible to record detailed bird migration routes and foraging trip tracks of
569 seabirds, and several species have been reported to compensate wind at sea. High-
570 resolution satellite-monitored GPS track data have demonstrated that juvenile ospreys
571 have been shown to be capable of wind compensation over open ocean spanning
572 distances in excess of 1,500 km [75]. By using satellite tracking, [76] documented the
573 northward migration tracks of 25 Hudson's Hudsonian godwits over 7,000 km from
574 Chiloé Island, Chile to the northern coast of the Gulf of Mexico, flying primarily over the
575 sea and revealed a strong preference for complete compensation throughout the entire
576 route of the godwits.

577 Wind compensation should have a significant impact on fitness not only in these
578 birds that migrate over the sea, but also in seabirds that fly over the sea throughout their
579 lives. During the breeding season, seabirds repeat foraging trips that travel hundreds of
580 kilometers from their breeding grounds to feeding sites at sea, and recent studies have
581 examined whether seabirds compensate for wind or drifted during their foraging trips
582 [68,71,73]. Antarctic petrels, *Pagodroma nivea*, nest on the Antarctic continent, and during
583 the breeding season they fly hundreds of kilometers over ice-covered land in strong
584 crosswinds to forage at sea. [73] investigated whether this species exhibits wind
585 compensation in the outward and return phases of foraging flights. The authors predicted
586 that wind compensation would be particularly strong on the return flight, as there is no
587 constraint to reach a specific foraging site on the outward flight, whereas there is a constraint
588 to reach a specific destination (nest) on the return flight. In the outbound phase, this species
589 showed partial compensation. However, contrary to expectations, the birds drifted during the
590 return phase, and the stronger the crosswind, the more the return path deviated from the
591 straight-line return path. In strong crosswinds (20 m/s), the return path was almost twice as
592 long as the straight-line distance to the nest. The authors suggest that this species is able to
593 compensate for crosswinds to some extent, and can achieve sufficient airspeed to
594 compensate, but that drift occurs because it is difficult to assess drift on the ice-covered
595 ground with few landmarks. [71] reported that streaked shearwaters compensate for
596 crosswinds over the sea during their homing to their nesting islands from foraging sites

597 located hundreds of kilometers away. Furthermore, their PDM at sea was oriented towards
598 the coast, deviating from their nesting island. This may indicate that they prioritise reliable
599 arrival at their destination over energy minimisation, and actively use the coast as a landmark,
600 because once a bird reaches the coast it can be sure to reach its nest by following the coast
601 line. [68] analyzed the homing routes of adult female and pre-fledging juvenile frigatebirds
602 flying over the sea, reporting that both groups compensate for wind, but adults exhibit a
603 stronger degree of compensation. Furthermore, the extent of juvenile compensation
604 increases with each successive trip, demonstrating the improvement of wind compensation
605 ability through experience. Additionally, juvenile frigatebirds showed a higher degree of
606 compensation when landmarks are visible suggesting that importance of landmarks for wind
607 compensation in young frigatebirds.

608 While these studies demonstrate that seabirds exhibit wind compensation to some
609 extent, it is interesting that these studies also reported that the degree of compensation gets
610 stronger in environments where landmarks are likely to be available [68,71]. Furthermore,
611 [71,73] pointed out the tendency that birds not to follow the shortest route straight back to
612 the nest, but to take a detour by first reaching the coast or mountain range near the goal and
613 then flying along them to return to the nest. One possible explanation for this is that the choice
614 of a route that, although long, is certain to reach the goal by using landmarks, i.e., not only
615 energy consumption but also the certainty of reaching the goal, may be a factor in the
616 currency of travel (we note that this strategy of prioritizing reaching a familiar point once over
617 the shortest route has been reported not only in flying seabirds but also in penguin homing
618 on land [77]). Another explanation is that drifting at the beginning and compensating at the
619 end of travel may consume less energy in response to changes in the wind environment to
620 reach the goal (the two possibilities are not exclusive). Testing the latter possibility requires
621 finding the optimal route in a spatiotemporally varying wind environment, which is the route
622 selection problem that will be discussed in the next section.

623

624 **5. Path Planning and Distribution in Response to Wind**

625 The studies that examined orientation in the previous sections either focus only on the
626 Heading direction at a given time or implicitly assume that the wind environment does not
627 change significantly until the goal. However, if the wind environment changes considerably
628 during travel, the bird needs to vary orientation over time to reduce travel costs. In this section,
629 we examine route selection under such conditions.

630

631 **5.1 Qualitative Prediction of Optimal Route Selection in Response to Wind**

632 Now we will examine an example of how spatial variation in wind changes the route that

633 minimizes the cost of travel. We simplify the setting of eq(9) and assume that the bird's
 634 airspeed is constant, i.e., ignoring airspeed adjustment and only focus on the heading
 635 adjustment, and that the bird adopts time instead of COT as its travel cost. The route that
 636 minimizes the travel time is then given by the following equation [64,78].

637

$$638 \quad \frac{d\theta}{dt} = -\left(\frac{du_w}{dx} - \frac{dv_w}{dy}\right) \cos\theta \sin\theta + \frac{du_w}{dy} \sin^2\theta - \frac{dv_w}{dx} \cos^2\theta \quad (24)$$

639

640 where θ is the Heading angle, which is the angle clockwise with respect to the y-axis.
 641 With the x-axis in the east and the y-axis in the north direction, consider a situation where
 642 the wind speed follows $(u_w, v_w) = (-Wy, 0)$ [m/s] between two points A, $(x, y) = (0, 0)$ [m], and
 643 B, $(x, y) = (0, 10^4)$ [m], 1.0×10^4 m apart, i.e., the wind speed gets faster as it goes north.
 644 Fig. 5 shows the routes given by Eq. (24) for the cases of starting from point A and arriving
 645 at B and starting from B and arriving at A, when $W = 8.0 \times 10^{-4}$, and 1.2×10^{-3} and the
 646 bird's airspeed is 8 m/s. When there is no wind, the straight-line route is the optimal.
 647 When traveling from south to north, the optimal route is to move upwind by
 648 overcompensation in the first part of the trip, and then to partially drift in the latter part of
 649 the trip (arrows from A to B in Fig. 5). On the other hand, when moving from north to
 650 south, i.e., when the wind becomes weaker as the goal gets closer, the optimal route is
 651 to partially drift in the first part of the trip and then correct for the deviation from the goal
 652 by overcompensation in the area where the wind becomes weaker in the latter part of
 653 the trip (arrows from B to A in Fig. 5). Hence, qualitative predictions derived from theory,
 654 i.e., the strategy of "using wind assistance by drift in areas of strong winds and
 655 compensating wind in areas with weak winds".

656 This prediction have also been reported in actual bird migrations [69,79]. [64]
 657 found that European honey buzzards, which breed in the Netherlands in the spring and
 658 overwinter in West Africa in the winter, take detours when traveling between breeding
 659 and wintering grounds, and that these routes differ between spring and winter as a result
 660 of route selection in response to wind. The study recorded spring and autumn migrations
 661 at one-hour sampling intervals to investigate how orientations vary with geographic
 662 position during migration. During the autumn migration from the Netherlands to Africa,
 663 honey buzzards moved southeastward, overcompensating for westward winds near the
 664 Atlas Mountains in northern Africa, and then over-drifted by southwestward winds in the
 665 Sahara. In contrast, during the spring migration, honey buzzard overcompensated for
 666 the eastward winds when departing East Africa and then over-drifted with north-westward
 667 wind in the Sahel region and the north-eastward winds in the Sahara, gaining tailwind

668 assistance. In other words, honey buzzards are expected to select their migration route
669 so that they can efficiently take advantage of the prevailing winds. While it has been
670 known that some birds take detour routes and/or different routes during spring and fall
671 migrations, [69] empirically demonstrated that the wind environment contributes to the
672 occurrence of the detour routes.

673

674 **5.2 Numerical Calculation of Optimal Routes in the Wind and Comparison with** 675 **Real Data**

676 So far, we have presented qualitative predictions on optimal route selection in response
677 to wind and their examination with real data. However, it would be useful as a further
678 analysis to calculate a route that minimizes COT based on wind information in the field
679 in accordance with the formulation of Equation (24) and compare it with real track data.
680 Specific methods for obtaining such routes include the Dijkstra algorithm [80] and the
681 numerical calculation of Zermelo's solution [81]. These methods provide a route that
682 minimizes the objective function (COT), assuming that the animal has a complete
683 knowledge of the spatio-temporal pattern of the wind environment until the goal. It should
684 be noted that the Dijkstra algorithm discretizes space, and therefore the travel direction
685 should be discretized, but it has the advantage of easy implementation. On the other
686 hand, the method of numerically computing Zermelo's solution has the advantage of
687 allowing travel direction to be treated as a continuous variable, although the
688 implementation of the computation is more complex than that of Dijkstra's algorithm.

689 [81] is, to the best of the authors' knowledge, the first study that compared the
690 numerically computed Zermelo solution with real-wildlife tracks (In this study, the
691 movement of animals is not to wind but to ocean currents, yet both can be treated in the
692 same framework since both are navigation in the flow). In this study, the migration tracks
693 of eight leatherback turtles that migrated approximately 1,000 km from their feeding sites
694 to the East African coast, where they laid their eggs, were calculated under the current
695 environment for the Zermelo solution and for two other migration strategies: vector
696 orientation (a strategy that maintains a constant heading direction from departure to goal)
697 and goal orientation (a strategy in which the heading angle is always oriented in the
698 direction of the goal) and compared them with real tracks of turtles. The results showed
699 that the Zermelo solution was less similar to the real routes than the other migration
700 strategies in seven individuals, although there was variability in the routes among the
701 individuals. In some individuals, the actual migration path was not similar to any of the
702 three theoretically computed paths. Especially three individuals showed a characteristic
703 pattern of large directional changes as they approached land at the end of their migration.

704 From these results, the authors conclude that turtles do not continually adjust their travel
705 direction relative to the target, but only orient themselves in the approximate direction to
706 the goal, and correction of their courses at the end of their migration is important for
707 reaching the goal. The Zermelo solution gives the solution with the minimum travel time,
708 i.e., the upper bound of the travel performance that the animal can achieve, assuming
709 that the animal has a perfect knowledge of the temporally varying flow. Therefore,
710 examining how the animal's actual path deviates from the optimal path, as shown in [81],
711 would provide insight into the animal's movement strategy and their navigation capacity.

712 It would also be useful to use the Zermelo solution as a benchmark for
713 evaluating the performance of other movement strategies [78]. By using the Zermelo
714 solution as a benchmark, [78] investigated whether simpler movement strategies than
715 the zermelo solution could achieve performance similar to the Zermelo solution. In [78],
716 two systems with very different travel distances were considered: thrushes' migration
717 over the North Sea from Norway to the Netherlands, which is about 800 km, and great
718 snipe's nonstop intercontinental migration from Scandinavia to West Africa, which is
719 about 6,000 km. The routes were simulated with four migration strategies: Zermelo
720 solution, complete compensation, vector orientation, and goal orientation, and their
721 performance (probability of reaching the goal range and travel time) of these strategies
722 was evaluated. The results revealed that vector orientation showed almost the same
723 performance as the Zermelo solution for systems that travel short distances, while the
724 goal oriented strategy showed almost the same performance as the Zermelo solution for
725 long-distance travel systems. These results indicate that simpler movement strategies
726 than the Zermelo solution, such as goal orientation and vector orientation, can also
727 perform similarly to the Zermelo solution, and that the performance of each strategy
728 varies greatly depending on the distance traveled (i.e., the degree of change in wind
729 environment). Interestingly, as a related note to the previous orientation section,
730 complete compensation underperformed either vector orientation or goal orientation in
731 both the thrushes and great snip systems. Complete compensation was less likely to
732 reach the goal in the thrushes system due to strong crosswinds encountered that could
733 not be compensated by the bird's airspeed, and in the great snip system, both the travel
734 time was longer and probability to reach the goal were lower than that of the goal
735 orientation strategy. This result is a good example of showing complete compensation is
736 not always the optimal path for long-distance migration due to upper limits on bird
737 airspeed and wind variation.

738 In light of the above, the Dijkstra algorithm and Zermelo's solution method may
739 be effective in the future in terms of providing an indication of the optimal path that can

740 be taken by the animal. These methods assume that the bird has a complete knowledge
741 of the spatio-temporal changes in the wind environment, but the extent to which the bird
742 is actually aware of the surrounding wind environment is an interesting topic in its own
743 right. In the future, it may be useful to estimate the extent to which birds are aware of the
744 surrounding wind environment based on actual path deviations from the Zermelo solution,
745 or to construct a more direct path planning calculation method that incorporates
746 uncertainty in the birds' knowledge of the wind environment.

747

748 **6 Future Issues**

749 We have reviewed three layers of bird movement strategies in response to wind:
750 movement mechanism, travel speed and orientation, and route selection. In this article,
751 we focused on the optimization problem of minimizing COT, a rather classic topic in bird
752 movement strategies. However, when examining real animal movements, deviations
753 from the optimal solution predicted by theory are often observed. This discrepancy
754 between theory and observations provides a starting point for new and exciting research.

755 For example, in this review, we assumed that COT is the currency of travel, i.e.,
756 the amount that an animal tries to minimize during its travels. In reality, however, it is
757 possible that costs other than COT are employed or that multiple factors contribute to
758 the currency of travel. One of these factors that has been attracting attention in recent
759 years is the risk of extra movement costs due to fluctuations in the environment that birds
760 cannot predict. Both the speed and the orientation adjustment and route selection that
761 minimize the COT presented in this article assume that the animal has a perfect
762 knowledge of the wind environment. In reality, however, the wind environment varies over
763 a variety of spatio-temporal scales. Therefore, a movement strategy that is expected to
764 minimize COT may require extra energy due to unexpected changes in the wind
765 environment. In other words, movement strategies that minimize COT are not robust to
766 fluctuations in the wind environment. The importance of the information birds have about
767 the wind environment on their movement decisions has been recently pointed out, and
768 recent bio-logging data allow for quantitative discussions [36,82]. In addition, the degree
769 to which birds are aware of their environment will vary depending on the experience of
770 each individual bird and the exchange of information in the flock[83]. In recent years, it
771 has become possible to collect movement data from individuals of various ages, and
772 differences in movement strategies by age have been reported for a variety of species
773 [68,82,84,85]. In addition, some studies have also examined the flow of information
774 within a flock [86,87].

775 Thus, due in part to the rapid improvement in the quality and quantity of bio-

776 logging data in recent years, we can expect to see further development in animal
777 movement strategy research in the future. A key to this development, along with
778 technology, will be the theory that provides a hypothesis to be tested. This review
779 presented several classic testing hypotheses of bird response to wind, all of which are
780 derived from a deterministic model. Real bird movement incorporates stochastic aspects,
781 both in the environment encountered and in the decision-making process. We believe
782 that the implementation of a stochastic model is useful for obtaining test hypotheses on
783 bird decision making in stochastic environments. In the past, ideas from the field of
784 statistical physics have often provided the springboard for new research topics in
785 movement ecology. For example, the application of statistical physics to animal flock
786 dynamics is a prominent research area [86–96]. As another example, the Levy Flight
787 Hypothesis, suggesting that animals maximize their food search efficiency by adopting
788 Levy Flights under conditions where prey density is low and prey distribution is
789 unpredictable, has sparked considerable research and debate [97–103]. These topics are
790 outside the scope of this paper; interested readers can find further information in the
791 references. We hope this paper will inspire physicists interested in movement ecology,
792 and catalyze research that integrates the theories and methodologies of physics and
793 ecology.

794

795 **Acknowledgement**

796 This study was financially supported by Grants-in-Aid for Scientific Research from the
797 Japan Society for the Promotion of Science (21H05294 and 22H00569).

798

799

- 800 1. Gray J. Studies in animal locomotion: VI. The propulsive powers of the dolphin. *J Exp*
801 *Biol.* 1936;13: 192–199.
- 802 2. Ellington CP. The aerodynamics of hovering insect flight. I. The quasi-steady analysis.
803 *Philos Trans R Soc Lond.* 1984;305: 1–15.
- 804 3. Ellington CP, van den Berg C, Willmott AP, Thomas ALR. Leading-edge vortices in insect
805 flight. *Nature.* 1996;384: 626–630.
- 806 4. Azuma A, Watanabe T. Flight performance of a dragonfly. *J Exp Biol.* 1988;137: 221–
807 252.

- 808 5. Farley CT, Glasheen J, McMahon TA. Running springs: speed and animal size. *J Exp*
809 *Biol.* 1993;185: 71–86.
- 810 6. Videler JJ, Stamhuis EJ, Povel GDE. Leading-edge vortex lifts swifts. *Science.*
811 2004;306: 1960–1962.
- 812 7. Nathan R, Getz WM, Revilla E, Holyoak M, Kadmon R, Saltz D, et al. A movement
813 ecology paradigm for unifying organismal movement research. *Proc Natl Acad Sci U S*
814 *A.* 2008;105: 19052–19059.
- 815 8. Shepard ELC, Wilson RP, Rees WG, Grundy E, Lambertucci SA, Vosper SB. Energy
816 landscapes shape animal movement ecology. *Am Nat.* 2013;182: 298–312.
- 817 9. McFarland DJ. Decision making in animals. *Nature.* 1977;269: 15–21.
- 818 10. Smith JM. Optimization Theory in Evolution. *Annu Rev Ecol Syst.* 1978;9: 31–56.
- 819 11. Stephens DW, Krebs JR. Foraging Theory. Princeton University Press; 1986.
- 820 12. Houston A, Clark C, McNamara J, Mangel M. Dynamic models in behavioural and
821 evolutionary ecology. *Nature.* 1988;332: 29–34.
- 822 13. Alerstam T. Optimal use of wind by migrating birds: combined drift and
823 overcompensation. *J Theor Biol.* 1979;79: 341–353.
- 824 14. Alerstam T. Wind as Selective Agent in Bird Migration. *Ornis Scand.* 1979;10: 76–93.
- 825 15. Alterstam T, Ulfstrand S. A Radar Study of the Autumn Migration of Wood Pigeons
826 *Columba Palumbus* in Southern Scandinavia. *Ibis.* 1974;116: 522–42.
- 827 16. Alerstam T. Crane *Grus Grus* migration over sea and land. *Ibis.* 1975;117: 489–495.
- 828 17. Jouventin P, Weimerskirch H. Satellite tracking of Wandering albatrosses. *Nature.*
829 1990;343: 746–748.
- 830 18. Higuchi H, Ozaki K, Fujita G, Minton J, Ueta M, Soma M, et al. Satellite tracking of white-
831 naped crane migration and the importance of the Korean demilitarized zone. *Conserv*
832 *Biol.* 1996;10: 806–812.
- 833 19. Yoda K, Naito Y, Sato K, Takahashi A, Nishikawa J, Ropert-Coudert Y, et al. A new
834 technique for monitoring the behaviour of free-ranging Adélie penguins. *J Exp Biol.*
835 2001;204: 685–690.

- 836 20. Yoda K, Sato K, Niizuma Y, Kurita M, Bost C, Le Maho Y, et al. Precise monitoring of
837 porpoising behaviour of Adélie penguins determined using acceleration data loggers. *J*
838 *Exp Biol.* 1999;202: 3121–3126.
- 839 21. Sakamoto KQ, Takahashi A, Iwata T, Trathan PN. From the Eye of the Albatrosses: A
840 Bird-Borne Camera Shows an Association between Albatrosses and a Killer Whale in
841 the Southern Ocean. *PLoS One.* 2009;4: e7322.
- 842 22. Rutz C, Bluff LA, Weir AAS, Kacelnik A. Video cameras on wild birds. *Science.* 2007;318:
843 765.
- 844 23. Takahashi A, Sato K, Naito Y, Dunn MJ, Trathan PN, Croxall JP. Penguin-mounted
845 cameras glimpse underwater group behaviour. *Proceedings of the Royal society B.* 2004.
846 Available: <https://royalsocietypublishing.org/doi/abs/10.1098/rsbl.2004.0182>
- 847 24. Yamamoto T, Kohno H, Mizutani A, Sato H, Yamagishi H, Fujii Y, et al. Effect of wind on
848 the flight of Brown Booby fledglings. *Ornithol Sci.* 2017;16: 17–22.
- 849 25. Williams HJ, Duriez O, Holton MD, Dell’Omo G, Wilson RP, Shepard ELC. Vultures
850 respond to challenges of near-ground thermal soaring by varying bank angle. *J Exp Biol.*
851 2018;221. doi:10.1242/jeb.174995
- 852 26. Naruoka M, Goto Y, Weimerskirch H. Application of Inertial and GNSS Integrated
853 Navigation to Seabird Biologging. *Journal of Robotics.* 2021. Available:
854 https://www.jstage.jst.go.jp/article/jrobomech/33/3/33_526/_article/-char/ja/
- 855 27. Schoombie S, Schoombie J, Brink CW, Stevens KL, Jones CW, Risi MM, et al.
856 Automated extraction of bank angles from bird - borne video footage using open -
857 source software. *J Field Ornithol.* 2019;90: 361-372.
- 858 28. Weimerskirch H, Guionnet T, Martin J, Shaffer SA, Costa DP. Fast and fuel efficient?
859 Optimal use of wind by flying albatrosses. *Proc Biol Sci.* 2000;267: 1869–1874.
- 860 29. Sakamoto KQ, Takahashi A, Iwata T, Yamamoto T, Yamamoto M, Trathan PN. Heart rate
861 and estimated energy expenditure of flapping and gliding in black-browed albatrosses.
862 *J Exp Biol.* 2013;216: 3175–3182.
- 863 30. Rattenborg NC, Voirin B, Cruz SM, Tisdale R, Dell’Omo G, Lipp H-P, et al. Evidence that
864 birds sleep in mid-flight. *Nat Commun.* 2016;7: 12468.
- 865 31. Takahashi S, Hombe T, Matsumoto S, Ide K, Yoda K. Head direction cells in a migratory

- 866 bird prefer north. *Sci Adv.* 2022;8: eabl6848.
- 867 32. Chapman JW, Klaassen RHG, Drake VA, Fossette S, Hays GC, Metcalfe JD, et al.
868 Animal orientation strategies for movement in flows. *Curr Biol.* 2011;21: R861-70.
- 869 33. Kempton JA, Wynn J, Bond S, Evry J, Fayet AL, Gillies N, et al. Optimization of dynamic
870 soaring in a flap-gliding seabird affects its large-scale distribution at sea. *Sci Adv.* 2022;8:
871 eabo0200.
- 872 34. Pennycuik CJ. Thermal soaring compared in three dissimilar tropical bird species,
873 *Fregata magnificens*, *Pelecanus occidentalis* and *Coragyps atratus*. *J Exp Biol.*
874 1983;102: 307–325.
- 875 35. Akos Z, Nagy M, Vicsek T. Comparing bird and human soaring strategies. *Proc Natl*
876 *Acad Sci U S A.* 2008;105: 4139–4143.
- 877 36. Horvitz N, Sapir N, Liechti F, Avissar R, Mahrer I, Nathan R. The gliding speed of
878 migrating birds: slow and safe or fast and risky? *Ecol Lett.* 2014;17: 670–679.
- 879 37. Rayleigh, Lord. The soaring of birds. *Nature.* 1883;27: 534–535.
- 880 38. Sachs G. Minimum shear wind strength required for dynamic soaring of albatrosses. *Ibis.*
881 2005;147: 1–10.
- 882 39. Richardson PL. How do albatrosses fly around the world without flapping their wings?
883 *Prog Oceanogr.* 2011;88: 46–58.
- 884 40. Bousquet GD, Triantafyllou MS, Slotine J-JE. Optimal dynamic soaring consists of
885 successive shallow arcs. *J R Soc Interface.* 2017;14. doi:10.1098/rsif.2017.0496
- 886 41. Richardson PL. Leonardo da Vinci's discovery of the dynamic soaring by birds in wind
887 shear. *Notes and Records: the Royal Society Journal of the History of Science.* 2019;73:
888 285–301.
- 889 42. Pokhrel S, Eisa SA. A novel hypothesis for how albatrosses optimize their flight physics
890 in real time: an extremum seeking model and control for dynamic soaring. *Bioinspir*
891 *Biomim.* 2022 [cited 7 Dec 2022]. doi:10.1088/1748-3190/aca5d9
- 892 43. Taylor GK, Reynolds KV, Thomas ALR. Soaring energetics and glide performance in a
893 moving atmosphere. *Philos Trans R Soc Lond B Biol Sci.* 2016;371.
894 doi:10.1098/rstb.2015.0398

- 895 44. Pennycuik CJ. *Modelling the Flying Bird*. Elsevier; 2008.
- 896 45. Goto Y, Yoda K, Weimerskirch H, Sato K. How did extinct giant birds and pterosaurs fly?
897 A comprehensive modeling approach to evaluate soaring performance. *PNAS Nexus*.
898 2022. doi:10.1093/pnasnexus/pgac023
- 899 46. Videler JJ. *Avian Flight*. OUP Oxford; 2006.
- 900 47. Norberg UM. *Vertebrate Flight: Mechanics, Physiology, Morphology, Ecology and*
901 *Evolution*. Springer Science & Business Media; 2012.
- 902 48. Klein Heerenbrink M, Johansson LC, Hedenström A. Power of the wingbeat: modelling
903 the effects of flapping wings in vertebrate flight. *Proceedings of the Royal Society A:*
904 *Mathematical, Physical and Engineering Sciences*. 2015;471: 20140952.
- 905 49. Tobalske BW, Hedrick TL, Dial KP, Biewener AA. Comparative power curves in bird flight.
906 *Nature*. 2003;421: 363–366.
- 907 50. Spedding GR, Rosén M, Hedenström A. A family of vortex wakes generated by a thrush
908 nightingale in free flight in a wind tunnel over its entire natural range of flight speeds. *J*
909 *Exp Biol*. 2003;206: 2313–2344.
- 910 51. Spedding GR, Hedenström A, Rosén M. Quantitative studies of the wakes of freely flying
911 birds in a low-turbulence wind tunnel. *Exp Fluids*. 2003;34: 291–303.
- 912 52. Muijres FT, Johansson LC, Bowlin MS, Winter Y, Hedenström A. Comparing
913 aerodynamic efficiency in birds and bats suggests better flight performance in birds.
914 *PLoS One*. 2012;7: e37335.
- 915 53. Johansson LC, Maeda M, Henningsson P, Hedenström A. Mechanical power curve
916 measured in the wake of pied flycatchers indicates modulation of parasite power across
917 flight speeds. *J R Soc Interface*. 2018;15. doi:10.1098/rsif.2017.0814
- 918 54. Warfvinge K, KleinHeerenbrink M, Hedenström A. The power–speed relationship is U-
919 shaped in two free-flying hawkmoths (*Manduca sexta*). *Journal of the Royal*. 2017.
920 Available: <https://royalsocietypublishing.org/doi/abs/10.1098/rsif.2017.0372>
- 921 55. Watanabe YY, Takahashi A, Sato K, Viviant M, Bost C-A. Poor flight performance in
922 deep-diving cormorants. *J Exp Biol*. 2011;214: 412–421.
- 923 56. Liechti F, Hedenström A, Alerstam T. Effects of Sidewinds on Optimal Flight Speed of

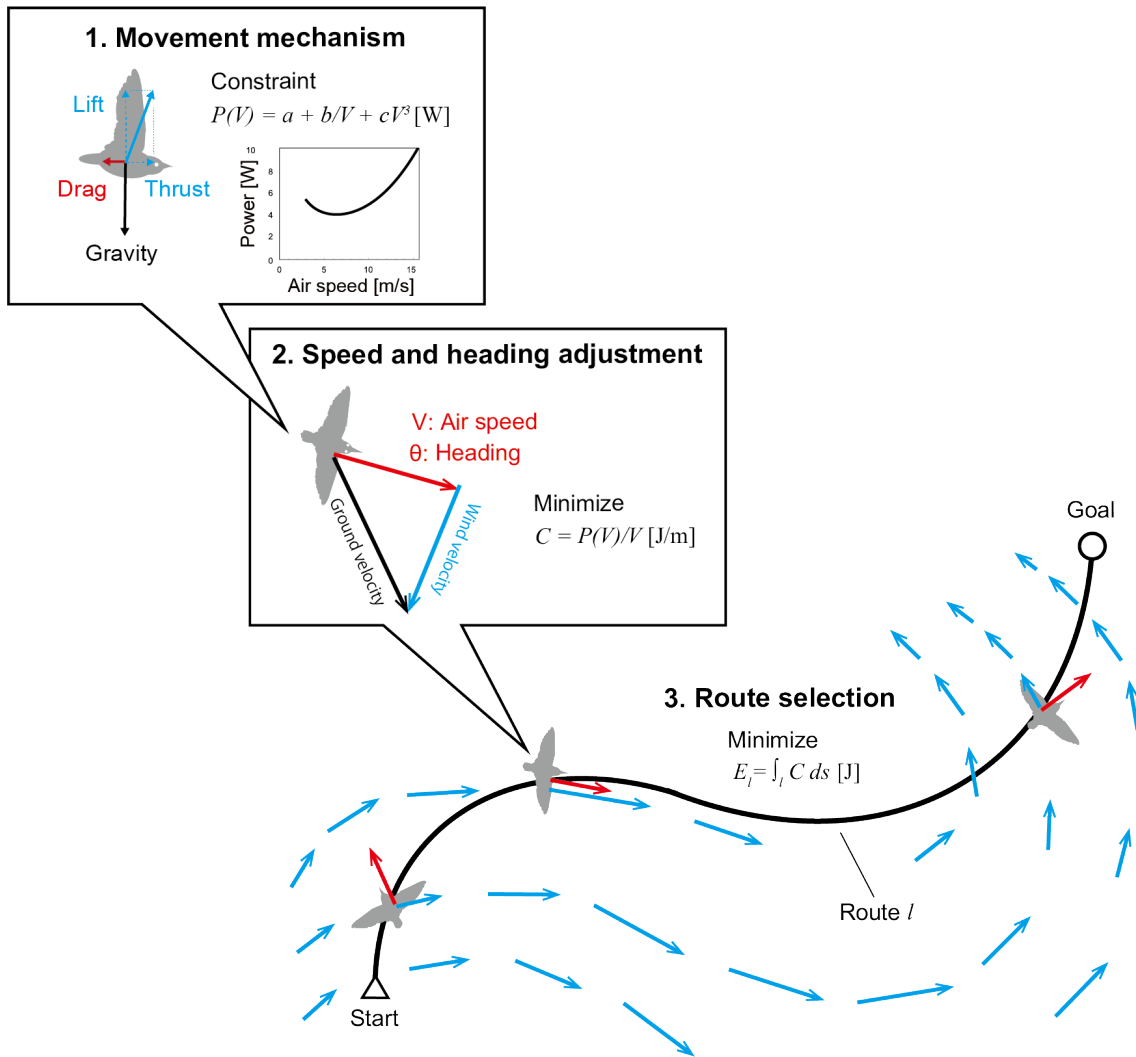
- 924 Birds. *J Theor Biol.* 1994;170: 219–225.
- 925 57. Hedenström A, Alerstam T, Green M, Gudmundsson GA. Adaptive variation of airspeed
926 in relation to wind, altitude and climb rate by migrating birds in the Arctic. *Behav Ecol*
927 *Sociobiol.* 2002;52: 308–317.
- 928 58. Hedenström A, Åkesson S. Ecology of tern flight in relation to wind, topography and
929 aerodynamic theory. *Philos Trans R Soc Lond B Biol Sci.* 2016;371.
930 doi:10.1098/rstb.2015.0396
- 931 59. Collins PM, Green JA, Elliott KH, Shaw PJA, Chivers L, Hatch SA, et al. Coping with the
932 commute: behavioural responses to wind conditions in a foraging seabird. *J Avian Biol.*
933 2020;51. doi:10.1111/jav.02057
- 934 60. Kogure Y, Sato K, Watanuki Y, Wanless S, Daunt F. European shags optimize their flight
935 behavior according to wind conditions. *J Exp Biol.* 2016;219: 311–318.
- 936 61. Karlsson H, Henningsson P, Bäckman J, Hedenström A, Alerstam T. Compensation for
937 wind drift by migrating swifts. *Anim Behav.* 2010;80: 399–404.
- 938 62. Sapir N, Horvitz N, Dechmann DKN, Fahr J, Wikelski M. Commuting fruit bats
939 beneficially modulate their flight in relation to wind. *Proc Biol Sci.* 2014;281: 20140018.
- 940 63. Hedenström A, Åkesson S. Adaptive airspeed adjustment and compensation for wind
941 drift in the common swift: differences between day and night. *Anim Behav.* 2017;127:
942 117–123.
- 943 64. Zermelo E. Über das Navigationsproblem bei ruhender oder veränderlicher
944 Windverteilung. *ZAMM Z Angew Math Mech.* 1931;11: 114–124.
- 945 65. Green M, Alerstam T. The problem of estimating wind drift in migrating birds. *J Theor*
946 *Biol.* 2002;218: 485–496.
- 947 66. Kemp MU, Shamoun-Baranes J, van Loon EE, McLaren JD, Dokter AM, Bouten W.
948 Quantifying flow-assistance and implications for movement research. *J Theor Biol.*
949 2012;308: 56–67.
- 950 67. Klaassen RHG, Hake M, Strandberg R, Alerstam T. Geographical and temporal flexibility
951 in the response to crosswinds by migrating raptors. *Proc Biol Sci.* 2011;278: 1339–1346.
- 952 68. Wynn J, Collet J, Prudor A, Corbeau A, Padget O, Guilford T, et al. Young frigatebirds

- 953 learn how to compensate for wind drift. *Proc Biol Sci.* 2020;287: 20201970.
- 954 69. Vansteelant WMG, Shamoun-Baranes J, van Manen W, van Diermen J, Bouten W.
955 Seasonal detours by soaring migrants shaped by wind regimes along the East Atlantic
956 Flyway. *J Anim Ecol.* 2017;86: 179–191.
- 957 70. Chapman JW, Nilsson C, Lim KS, Bäckman J, Reynolds DR, Alerstam T. Adaptive
958 strategies in nocturnally migrating insects and songbirds: contrasting responses to wind.
959 *J Anim Ecol.* 2016;85: 115–124.
- 960 71. Goto Y, Yoda K, Sato K. Asymmetry hidden in birds' tracks reveals wind, heading, and
961 orientation ability over the ocean. *Science advances.* 2017. Available:
962 <https://www.science.org/doi/abs/10.1126/sciadv.1700097>
- 963 72. Shiomi K, Sato K, Katsumata N, Yoda K. Temporal and spatial determinants of route
964 selection in homing seabirds. *Behaviour.* 2019;156: 1165–1183.
- 965 73. Tarrow A, Weimerskirch H, Wang S-H, Bromwich DH, Cherel Y, Kato A, et al. Flexible
966 flight response to challenging wind conditions in a commuting Antarctic seabird: do you
967 catch the drift? *Anim Behav.* 2016;113: 99–112.
- 968 74. Alerstam T, Ulfstrand S. A RADAR STUDY OF THE AUTUMN MIGRATION OF WOOD
969 PIGEONS COLUMBA PALUMBUS IN SOUTHERN SCANDINAVIA. *Ibis* . 1974.
970 doi:10.1111/j.1474-919X.1974.tb07649.x
- 971 75. Horton TW, Bierregaard RO, Zawar-Reza P, Holdaway RN, Sagar P. Juvenile Osprey
972 Navigation during Trans-Oceanic Migration. *PLoS One.* 2014;9: e114557.
- 973 76. Linscott JA, Navedo JG, Clements SJ, Loghry JP, Ruiz J, Ballard BM, et al.
974 Compensation for wind drift prevails for a shorebird on a long-distance, transoceanic
975 flight. *Mov Ecol.* 2022;10: 11.
- 976 77. Quintana F, Gómez-Laich A, Gunner RM, Gabelli F, Omo GD, Duarte C, et al. Long walk
977 home: Magellanic penguins have strategies that lead them to areas where they can
978 navigate most efficiently. *Proc Biol Sci.* 2022;289: 20220535.
- 979 78. McLaren JD, Shamoun-Baranes J, Dokter AM, Klaassen RHG, Bouten W. Optimal
980 orientation in flows: providing a benchmark for animal movement strategies. *J R Soc*
981 *Interface.* 2014;11. doi:10.1098/rsif.2014.0588
- 982 79. Vansteelant WMG, Gangoso L, Bouten W, Viana DS, Figuerola J. Adaptive drift and

- 983 barrier-avoidance by a fly-forage migrant along a climate-driven flyway. *Mov Ecol.*
984 2021;9: 37.
- 985 80. Kranstauber B, Weinzierl R, Wikelski M, Safi K. Global aerial flyways allow efficient
986 travelling. *Ecol Lett.* 2015;18: 1338–1345.
- 987 81. Hays GC, Christensen A, Fossette S, Schofield G, Talbot J, Mariani P. Route optimisation
988 and solving Zermelo’s navigation problem during long distance migration in cross flows.
989 *Ecol Lett.* 2014;17: 137–143.
- 990 82. Harel R, Horvitz N, Nathan R. Adult vultures outperform juveniles in challenging thermal
991 soaring conditions. *Sci Rep.* 2016;6: 27865.
- 992 83. Williams HJ, Safi K. Certainty and integration of options in animal movement. *Trends*
993 *Ecol Evol.* 2021;36: 990–999.
- 994 84. Yoda K, Yamamoto T, Suzuki H, Matsumoto S, Müller M, Yamamoto M. Compass
995 orientation drives naïve pelagic seabirds to cross mountain ranges. *Curr Biol.* 2017;27:
996 R1152–R1153.
- 997 85. Sergio F, Barbosa JM, Tanferna A, Silva R, Blas J, Hiraldo F. Compensation for wind drift
998 during raptor migration improves with age through mortality selection. *Nat Ecol Evol.*
999 2022;6: 989–997.
- 1000 86. Flack A, Nagy M, Fiedler W, Couzin ID, Wikelski M. From local collective behavior to
1001 global migratory patterns in white storks. *Science.* 2018;360: 911–914.
- 1002 87. Nagy M, Couzin ID, Fiedler W, Wikelski M, Flack A. Synchronization, coordination and
1003 collective sensing during thermalling flight of freely migrating white storks. *Philos Trans*
1004 *R Soc Lond B Biol Sci.* 2018;373. doi:10.1098/rstb.2017.0011
- 1005 88. Vicsek T, Czirók A, Ben-Jacob E, Cohen I I, Shochet O. Novel type of phase transition
1006 in a system of self-driven particles. *Phys Rev Lett.* 1995;75: 1226–1229.
- 1007 89. Couzin ID, Krause J, Franks NR, Levin SA. Effective leadership and decision-making in
1008 animal groups on the move. *Nature.* 2005;433: 513–516.
- 1009 90. Nagy M, Akos Z, Biro D, Vicsek T. Hierarchical group dynamics in pigeon flocks. *Nature.*
1010 2010;464: 890–893.
- 1011 91. Vicsek T, Zafeiris A. Collective motion. *Phys Rep.* 2012. Available:

- 1012 <https://www.sciencedirect.com/science/article/pii/S0370157312000968>
- 1013 92. Hayakawa Y, Furuhashi S. Group-size distribution of skeins of wild geese. *Phys Rev E*
1014 *Stat Nonlin Soft Matter Phys.* 2012;86: 031924.
- 1015 93. Yomosa M, Mizuguchi T, Hayakawa Y. Spatio-temporal structure of hooded gull flocks.
1016 *PLoS One.* 2013;8: e81754.
- 1017 94. Pettit B, Perna A, Biro D, Sumpter DJT. Interaction rules underlying group decisions in
1018 homing pigeons. *J R Soc Interface.* 2013;10: 20130529.
- 1019 95. Yomosa M, Mizuguchi T, Vásárhelyi G, Nagy M. Coordinated Behaviour in Pigeon Flocks.
1020 *PLoS One.* 2015;10: e0140558.
- 1021 96. Sridhar VH, Li L, Gorbonos D, Nagy M, Schell BR, Sorochkin T, et al. The geometry of
1022 decision-making in individuals and collectives. *Proc Natl Acad Sci U S A.* 2021;118.
1023 doi:10.1073/pnas.2102157118
- 1024 97. Viswanathan GM, Afanasyev V, Buldyrev SV, Murphy EJ, Prince PA, Stanley HE. Lévy
1025 flight search patterns of wandering albatrosses. *Nature.* 1996;381: 413–415.
- 1026 98. Viswanathan GM, Buldyrev SV, Havlin S, da Luz MG, Raposo EP, Stanley HE.
1027 Optimizing the success of random searches. *Nature.* 1999;401: 911–914.
- 1028 99. Sims DW, Southall EJ, Humphries NE, Hays GC, Bradshaw CJA, Pitchford JW, et al.
1029 Scaling laws of marine predator search behaviour. *Nature.* 2008;451: 1098–1102.
- 1030 100. Humphries NE, Queiroz N, Dyer JRM, Pade NG, Musyl MK, Schaefer KM, et al.
1031 Environmental context explains Lévy and Brownian movement patterns of marine
1032 predators. *Nature.* 2010;465: 1066–1069.
- 1033 101. Benhamou S, Collet J. Ultimate failure of the Lévy Foraging Hypothesis: Two-scale
1034 searching strategies outperform scale-free ones even when prey are scarce and cryptic.
1035 *J Theor Biol.* 2015;387: 221–227.
- 1036 102. Buchanan M. Confused at a higher level. *Nat Phys.* 2018;14: 1070–1070.
- 1037 103. Klages R. Search for Food of Birds, Fish, and Insects. In: Bunde A, Caro J, Chmelik
1038 C, Kärger J, Vogl G, editors. *Diffusive Spreading in Nature, Technology and Society.*
1039 Cham: Springer International Publishing; 2023. pp. 53–74.
- 1040

1041



1042

1043 **Figure 1. (Color online) The three hierarchies constituting animal movement**

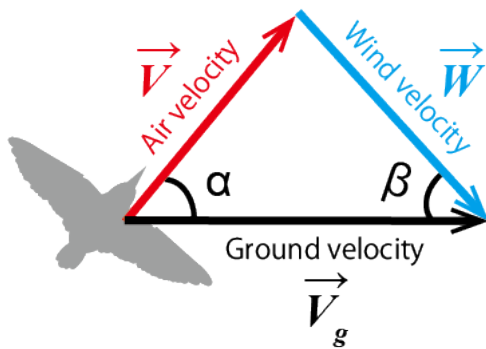
1044 Locomotion of animals is composed of three hierarchies. The micro-scale movement

1045 mechanism, the medium-scale adjustment of speed and heading, and the macro-scale

1046 route selection.

1047

1048



1049

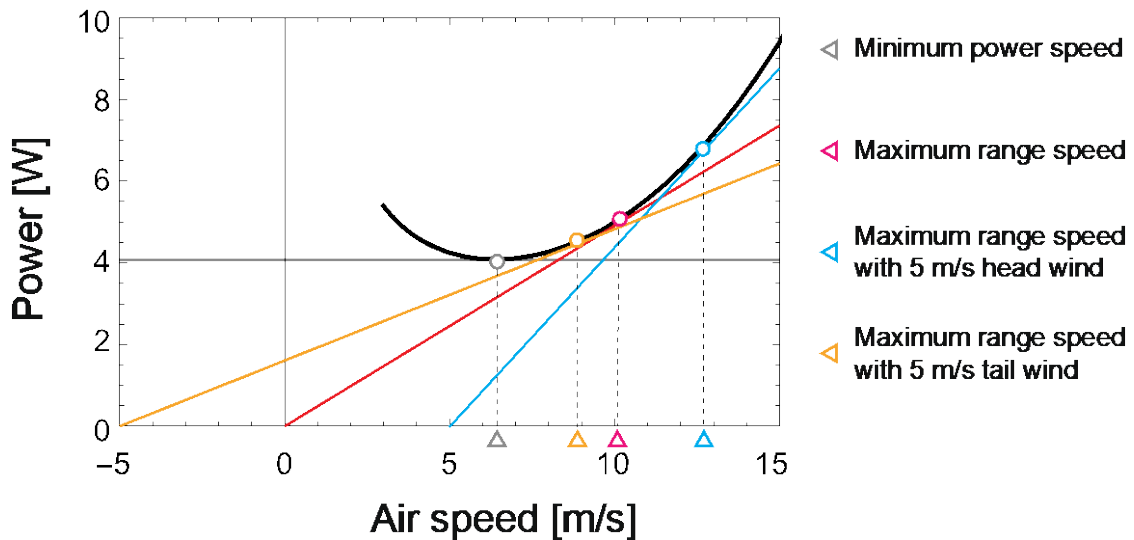
1050 **Figure2. (Color online) Air velocity and ground velocity**

1051 The ground velocity (black arrow) is the bird's velocity relative to the ground. The air

1052 velocity (red arrow) is the bird's velocity relative to the air. The blue arrow is the wind

1053 velocity. The ground velocity is the vector sum of the air velocity and the wind velocity.

1054



1055

1056 **Figure 3. (Color online) Power curve and maximum range speed**

1057 The black line represents the power curve. The minimum power speed is the airspeed at

1058 which the power is minimized (indicated by the gray triangle). The maximum range speed

1059 in no wind conditions is given by the tangent line drawn from the origin to the power curve

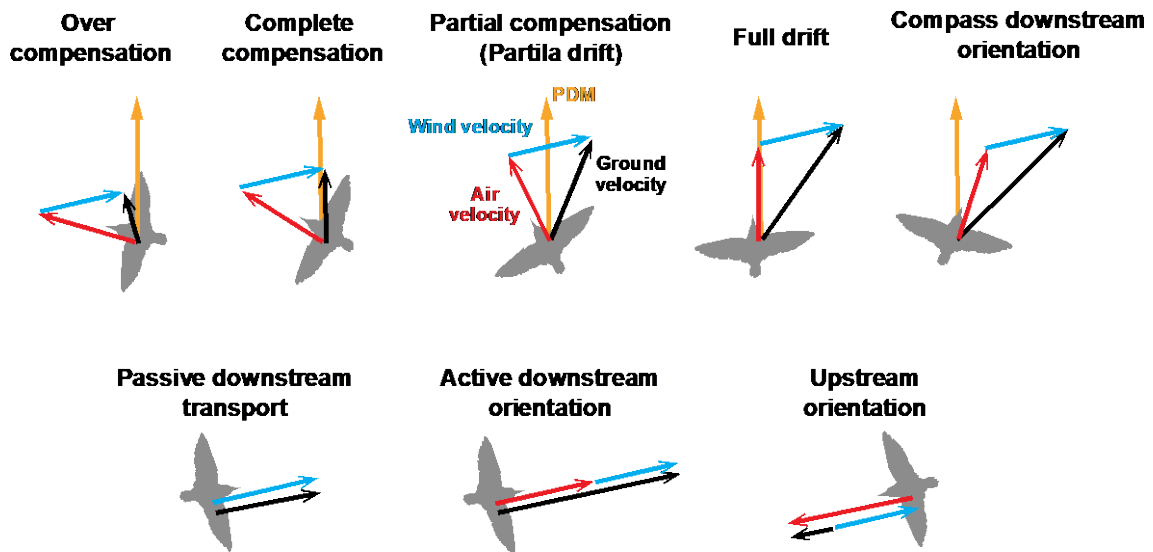
1060 (red triangle). The maximum range speed with a headwind of 5 m/s is given by the

1061 tangent drawn to the power curve from air speed = 5 [m/s] and power = 0 [W] (indicated

1062 by the blue triangle); the maximum range speed with a tailwind of 5 m/s is given by the

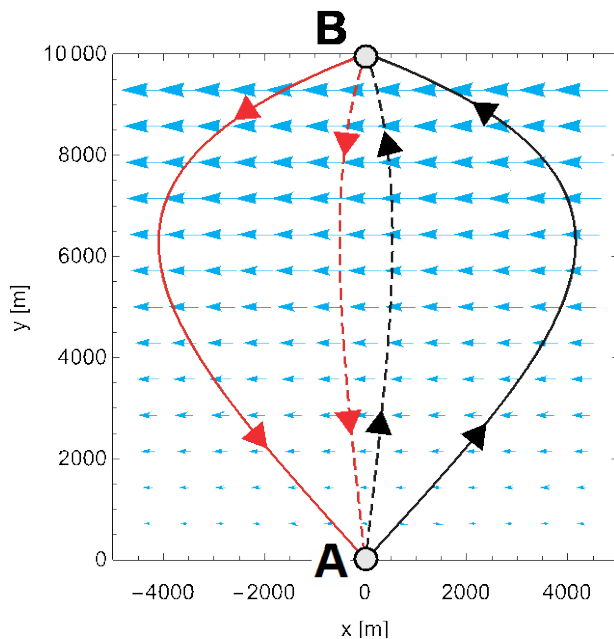
1063 tangent line drawn from air speed = -5 [m/s], power = 0 [W] to the power curve (indicated

1064 by the orange triangle).



1065
1066
1067
1068
1069

Figure 4 (Color online) Classification of orientations in response to the wind
Eight type of orientation of animals moving in flows proposed by Chapmann (2011)



1070
1071
1072
1073
1074
1075
1076
1077

Figure 5. (Color online) Optimal routes in spatially varying wind conditions
Time minimizing routes under the wind field that follows $(u_w, v_w) = (-Wy, 0)$ [m/s]. The blue arrows represent the wind velocities. The bird travels between two points A, $(x, y) = (0, 0)$ [m], and B, $(x, y) = (0, 10^4)$ [m]. The black lines are optimal route to travel from the point A to B with $W = 1.2 \times 10^{-3}$ (black solid line) and $W = 8.0 \times 10^{-4}$ (black dashed line). The red lines are optimal route to travel from the point B to A with $W = 1.2 \times 10^{-3}$ (red solid line) and $W = 8.0 \times 10^{-4}$ (red dashed line).

\vec{V}	Air velocity
V	Airspeed ($V \equiv \vec{V} $)
θ	The direction of the air velocity (Heading direction) ($\theta \equiv \arg \vec{V}$)
\vec{V}_g	Ground velocity
V_g	Ground speed ($V_g \equiv \vec{V}_g $)
\vec{W}	Wind velocity
W	Wind speed ($W \equiv \vec{W} $)
u_w	x component of the wind velocity
v_w	y component of the wind velocity

Table 1 Notation of symbols